On the use of a Stress-Impedance Model to describe sound propagation in a lined duct with grazing flow

Yves Aurégan

On the use of a Stress–Impedance Model to describe sound propagation in a lined duct with grazing flow

Yves Aurégan[1, *]

[1] *Laboratoire d'Acoustique de l'Université du Mans, Centre National de la Recherche Scientifique (CNRS), Le Mans Université, Avenue Olivier Messiaen, 72085 Le Mans Cedex 9, France*

(Dated: April 23, 2018)

With flow, the acoustic effect of a locally reacting lined wall cannot be described by a single quantity independent of the incident wave, such as a wall impedance. At least two quantities, intrinsic to the liner and to the flow, are required to describe the effect of the lined wall regardless of the incident wave. In addition to the impedance, the unsteady tangential force exerted by the wall on the flow has to be taken into account. This force is due either to viscous effects or to the unsteady transfer of axial momentum from the flow into the lined wall. The paper describes a Stress–Impedance model where the two variables used are the impedance and the friction factor that links the pressure to a tangential stress at the wall. The use of a wall stress helps to better understand the mechanisms of momentum transfer between the flow and the wall in the vicinity of an acoustic treatment.

I. INTRODUCTION

Despite its practical importance, the behavior of acoustic treatments in the presence of a grazing flow is still poorly understood. This is due to the complexity of the unsteady turbulent flow near the perforated plate holes that has been demonstrated by numerical simulations [16]. Most of the currently used models assume that the effect of the flow boundary layer can be described by the Ingard-Myers relation [5, 9] and that, for a locally reacting liner, the flow complexity can be captured by an equivalent impedance, independent of the incident wave, that must be empirically or semi-empirically determined.

Much work has been done to improve the description of the boundary layer effect [6]. Despite these advances, the commonly used models are still unable to explain the difference between the impedances deduced from measurements in the flow direction and in the opposite direction [2, 11, 15].

It has been shown in [10, 13, 14] that the oscillating shear stress can play an important role in sound propagation with a grazing flow along a liner. This shear stress is apparently due to the interaction between turbulent flow and the rough wall which is the interface of the acoustic treatment. Further attempts were made to account for shear stress in terms of viscous stress [1, 7] or in term of additional force acting on the walls of a cavity [8]. A modified boundary condition was derived that introduces a coefficient β_v that characterizes the transfer, by the normal fluctuating displacement, of axial momentum from the steady flow into the lined wall [1]. Another modified boundary condition was more recently derived that uses the momentum transfer impedance ζ_T [10, 13, 14].

In this paper, a heuristic approach is used: The existence of a tangential surface force on the wall is postulated and this paper describes how this force can be deduced from measurements or calculations. The detailed analysis of how this shear stress is created at the wall of the liner is outside the scope of this paper and is yet to be investigated.

The paper is organized as follows: Section II presents the Stress–Impedance model and a way of computing both the impedance and the stress, under the form of an equivalent friction factor, from the knowledge of two different wave numbers in a two-dimensional (2D) geometry. Section III presents the application of this model to the numerical simulations made in a 2D propagation problem [4].

II. THE STRESS–IMPEDANCE MODEL

A. General equations

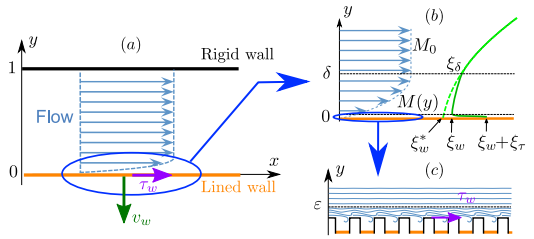

FIG. 1. (color online) General view of the 2D problem.

The propagation in a two–dimensional (2D) duct of height h with a shear flow of velocity $U(y)$ is considered. The velocity is supposed to be uniform outside of the boundary layer having a thickness δ and it decreases and then vanishes on the lower wall. On this wall, the duct is acoustically treated. The acoustic treatment is described classically by an admittance $Y_w = v_w/p_w$ that links the normal velocity into the wall v_w to the pressure

* yves.auregan@univ-lemans.fr

at the wall p_w but also by a tangential stress τ_w that is intended to describe an unsteady transfer of momentum from the flow into the wall due to wall roughness and to turbulent and viscous effects. Those effects are supposed to be confined near the wall in a layer of thickness ε smaller than the mean flow boundary layer δ, see Fig. 1. To simplify the notations, all parameters are nondimensionalized. All velocities are nondimensionalized by the speed of sound c_0, so that the mean velocity becomes the Mach number $M(y)$. Distances are nondimensionalized by the height of the channel h, time by h/c_0, and pressure by $\rho_0 c_0^2$ where ρ_0 is the mean density. Except very near the wall ($0 < y < \varepsilon$), all the dissipative effects can be neglected and the dimensionless equations governing the acoustic motion are

$$D_t u + M' v = -\partial_x p \tag{1}$$
$$D_t v = -\partial_y p \tag{2}$$
$$D_t p = -\partial_x u - \partial_y v \tag{3}$$

where u, v are respectively the velocities in the x and y direction, p is the pressure, $D_t = \partial_t + M\partial_x$ is the convective derivative and $M' = d_y M$. To avoid singular terms in the above equations when the boundary layer thickness vanishes, it is advantageous to rewrite Eqs. (1–3) only in terms of pressure p and transverse displacement ξ ($v = D_t\xi$) which are the regular variables in the boundary layer (those variables remain continuous when the boundary layer thickness vanishes):

$$\partial_y p = -D_t^2 \xi \tag{4}$$
$$D_t^2 \partial_y \xi = \partial_x^2 p - D_t^2 p \tag{5}$$

The pressure and the displacement are taken under the form $p(x,y,t) = \hat{p}(y)\exp(\mathrm{j}(\omega t - kx))$ and $\xi(x,y,t) = \hat{\xi}(y)\exp(\mathrm{j}(\omega t - kx))$ and Eqs. (4–5) become:

$$\mathrm{d}_y \hat{p} = \Omega^2 \hat{\xi} \tag{6}$$
$$\Omega^2 \mathrm{d}_y \hat{\xi} = k^2 \hat{p} - \Omega^2 \hat{p} \tag{7}$$

where $\Omega = \omega - kM(y)$. In the following, the hats are removed for simplicity.

B. Effect of the boundary layer

At the lowest order, when the boundary layer thickness is very small compared to the height of the channel ($\delta \ll 1$), Eqs. (6–7) show that $p_w = p_w^*$ and $\xi_w = \xi_w^*$ where p_w^* and ξ_w^* are the values at the wall when the flow is uniform up to the wall. At this level of approximation, the boundary layer only induces a jump in the normal velocity $\omega v_w^* = \Omega_0 v_w$ where $\Omega_0 = \omega - kM_0$ and M_0 is the Mach number in the uniform flow.

A more precise description [3], at the first order in δ, is obtained by integrating Eqs. (6–7) over the boundary layer, see Appendix A:

$$p_w - p_w^* = \delta\mathcal{I}_0 \Omega_0^2\, \xi_w \tag{8}$$
$$\xi_w - \xi_w^* = \delta\mathcal{I}_1 k^2/\Omega_0^2\, p_w \tag{9}$$

where

$$\delta\mathcal{I}_1 = \int_0^\delta 1 - \left(\frac{\Omega_0}{\Omega}\right)^2 \mathrm{d}y \quad \text{and} \quad \delta\mathcal{I}_0 = \int_0^\delta 1 - \left(\frac{\Omega}{\Omega_0}\right)^2 \mathrm{d}y$$

C. Stress along the wall

To study the near wall zone ($0 < y < \varepsilon$), the effect of a shear stress along the x direction is added to Eq. (7):

$$\Omega^2 \mathrm{d}_y \xi = k^2 p - \Omega^2 p - \mathrm{j}k\mathrm{d}_y \tau \tag{10}$$

By considering that the mean flow is very weak in the near wall zone and that $\varepsilon \ll 1$, this equation can be integrated along y in $\omega^2 \xi_\tau = -\mathrm{j}k\tau_w$ where τ_w is the stress at the wall and ξ_τ is an additional displacement due to the stress. It can be noted that this relation has to be modified (ω become $\omega - U_s k/c_0$) if a slip velocity U_s is considered at the wall to take into account the effect of the roughness on the turbulent motion [12].

D. Equivalent boundary condition

At the lowest order, when the thickness of the boundary layer δ is negligible, the relation between p_w^* and $v_w^* = \mathrm{j}\Omega_0 \xi_w^*$, pressure and normal velocity at the wall when a perfect uniform flow is considered, and p_w and $v_w = \mathrm{j}\omega(\xi_w^* + \xi_\tau)$, pressure and normal velocity at the wall when the boundary layer and the stress are considered, are

$$p_w^* = p_w \quad \text{and} \quad v_w^* = \frac{\Omega_0}{\omega} v_w - \frac{\Omega_0 k}{\omega^2}\tau_w \tag{11}$$

In this case, the equivalent admittance $Y_w^* = -v_w^*/p_w^*$ (seen by a wave propagating in a uniform flow) can be computed from the admittance of the wall ($Y_w = -v_w/p_w$) and f_w by

$$Y_w^* = \frac{\Omega_0}{\omega}\left(Y_w + \frac{k}{\omega} f_w\right) \tag{12}$$

where $f_w = \tau_w/p_w$ can be seen as an equivalent friction coefficient.

In the uniform flow, Eqs. (6–7) result in $\mathrm{d}_y^2 p = -\alpha^2 p$ where $\alpha^2 = \Omega_0^2 - k^2$. The pressure can be written $p = A\cos(\alpha(1-y))$ and, at the lined wall $y = 0$, the relation between pressure and velocity is $-v(0)/p(0) = Y_w^* = -\mathrm{j}\alpha\tan(\alpha)/\Omega_0$.

When two values of the wavenumber k are known, two values of Y_w^* can be computed and Eq. (12) can be used for the determination of the admittance Y_w and of the friction coefficient f_w. For a more precise solution, the influence of the boundary layer can be taken into account by [3]:

$$\left(1 + \frac{\mathrm{j}\Omega_0^2}{\omega}\delta\mathcal{I}_0 Y_w\right) Y_w^* = \frac{\Omega_0}{\omega}\left(Y_w + \frac{k}{\omega} f_w\right) + \mathrm{j}\frac{k^2}{\Omega_0}\delta\mathcal{I}_1 \tag{13}$$

E. Links with previous formulations

When the Ingard-Myers boundary condition is used without taking into account the surface force, Eq. (12) applies with $f_w = 0$. In some papers [1, 11], the Ingard-Myers condition has been modified by using a new parameter β_v and the relation between the normal velocity at the wall with an uniform flow v_w^* and the normal velocity in the liner v_w is transformed into $v_w^* = (1-(1-\beta_v)M_0 k/\omega)v_w$. Eq. (12) becomes:

$$Y_w^* = \frac{\Omega_0}{\omega} Y_\beta + \frac{kM_0}{\omega}\beta_v Y_\beta \tag{14}$$

In [13], the momentum transfer impedance $\zeta_T = -\tau_w/v_w$ is used. Using Eq. (12)

$$Y_w^* = \frac{\Omega_0}{\omega}\left(1 + \frac{k\zeta_T}{\omega}\right) Y_T \tag{15}$$

In general, the admittance Y_w extracted using the present Stress–Impedance model is not equal to the admittance Y_β extracted using the β_v–model or to the admittance Y_T extracted using the ζ_T–model. Thus the three formulations are not exactly equivalent and will give different results.

When only two values of the complex wavenumber k are known, they can always be described using two complex numbers such as Y_w and f_w, Y_β and β_v or Y_T and ζ_T. A true validation of these models can only be achieved when more than two wavenumbers are known. This can be done experimentally or numerically either by determining, at a given configuration, the higher order modes, which are generally strongly attenuated, or by increasing the channel size to have more propagating (or slightly attenuated) modes.

III. APPLICATION OF THE STRESS–IMPEDANCE MODEL

A. Numerical determination of the wavenumbers

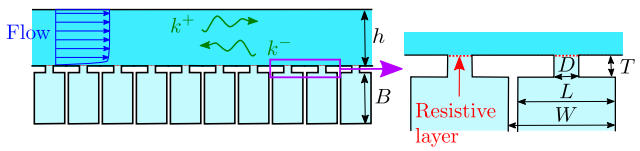

FIG. 2. (color online) Sketch of an array of 2D periodic cells with Helmholtz resonators.

The linear acoustic propagation with flow is computed in an array of 2D periodic cells with Helmholtz resonators, see Fig. 2. Neglecting the viscous and thermal losses, the linearized Euler equations are solved in one of the periodic cells by using the multimodal method as described in [4]. In the numerical calculation, the geometry is defined by the height of the duct $h = 15$ mm, the depth of the resonator cavity $B = 25$ mm, the period between two resonators which is equal to the width of the cavity $W = L = 5$ mm, the thickness of the resonator neck $T = 0.5$ mm and the width of the hole $D = 1$ mm. With those dimensions, the resonance frequency of the Helmholtz resonators is 2700 Hz. A resistive layer has been added to insure some dissipation in the neck of the Helmholtz resonators and the normalized resistance is 0.05. A shear flow profile has been taken into account and the Mach number is given as a function of the mean Mach number M_0 by $M(y) = M_0(m+1)(1-(1-y)^m)/m$ where $m = 30$ to insure a small thickness of the boundary layer.

The output of the numerical calculations is a transmission matrix that links all the modes at the entrance of one cell to the modes at the exit of this cell. In the present calculation, 900 modes been considered. Using the Floquet-Bloch approach, the wavenumbers in the periodic system are computed and the wavenumbers of the least attenuated modes in each propagation direction k_B^+ and k_B^- are selected and will be used in the following to compute the impedance and the friction coefficient f_w. The value of k_B^+ and k_B^- are plotted in Fig 3.

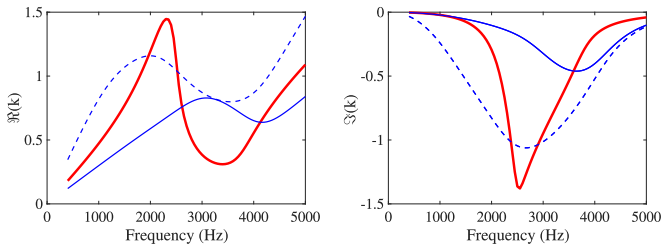

FIG. 3. (color online) Real and imaginary values of the dimensionless wavenumbers k_B^+ (continuous lines) and $-k_B^-$ (dashed lines) without flow (thick red curve) and with flow ($M_0 = 0.3$, in blue). Without flow $k_B^+ = -k_B^-$.

B. Impedance and friction factor

When the boundary layer effect is neglected, Eq. (12) is written, using $k = k_B^+$ and $k = k_B^-$,

$$Y^\pm = Y_w + k_B^\pm f_w/\omega \tag{16}$$

where $Y^\pm = -\mathrm{j}\omega\alpha^\pm \tan(\alpha^\pm)/(\Omega_0^\pm)^2$. The two Eqs. (16) allow the determination of Y_w and f_w. The value of the dimensionless impedance of the plate is computed by removing the effect of the cavity from the impedance of the resonator: $Z_w = 1/Y_w + \mathrm{j}/\tan(\omega B)$. It is plotted in Fig 4 and compared to the two values $Z^\pm$ obtained from $Y^\pm$ by assuming $f_w = 0$ in Eq. (16). Without flow, the three values of the impedance are equal. The real part is almost constant and equal to the resistance of the dissipative layer divided by the percentage of open area.

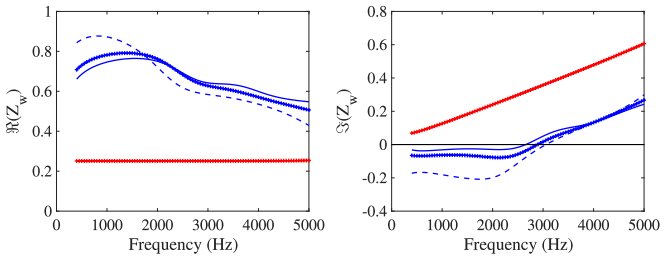

FIG. 4. (color online) Real and imaginary values of the equivalent impedance without flow (in red) and with flow ($M_0 = 0.3$, in blue). The symbols represents the value computed with the Stress–Impedance model, the continuous line (resp. dashed line) is the value obtained by considering $f_w = 0$ from k_B^+ (resp. k_B^-).

The imaginary part increases linearly with the frequency and is related to the mass of fluid moving in the hole and its vicinity. With flow, the two impedances $Z^\pm$ deduced by assuming $f_w = 0$ are different showing again that the equivalent impedance depends on the direction of the incident waves in the classical approach [4]. On the contrary, the impedance is determined in a unique way in the Stress–Impedance model.

The additional effect, which is supposed to describe the difference between impedances with different wave incidences (i. e. different values of k), is the tangential force acting on the lined wall. It is described by the friction coefficient f_w which is plotted in Fig 5.

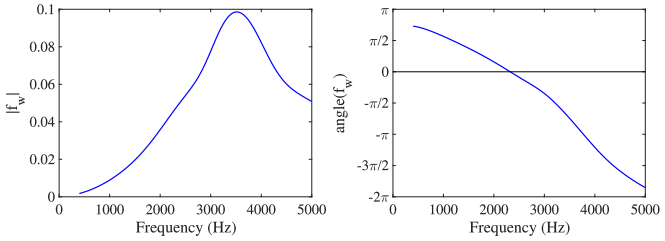

FIG. 5. (color online) Modulus and phase of the friction coefficient f_w in the case with flow ($M_0 = 0.3$).

The amplitude of the friction coefficient starts from 0 and increases to reach a maximum amplitude at 3.5 kHZ, which is slightly higher than the resonance frequency of Helmholtz resonators with flow (3.3 kHz). The phase of the friction coefficient indicates that stress and pressure are in opposition of phase at low frequencies. The phase decreases regularly and the opposition of phase occurs again at 3.8 kHz. This indicates that there is a characteristic time delay (0.26 ms) between stress and pressure. Looking at Fig 6, it can be thought that a part of this stress comes from the unsteady force applied to the vertical walls of holes by an hydrodynamic mode that is created at the level of the upstream wall and that is convected and amplified. This convection time may explain the delay between stress and pressure. However, the results of the numerical simulation should be interpreted with caution because an artificial damping of the hydrodynamic modes has been added near the rigid wall to mimic the destruction of coherent structures by turbulence (see Fig. 3 in [4]). This damping results in an artificial change in momentum along the x direction. A more precise numerical simulations (possibly including turbulence, viscous and thermal effects) will have to be carried out to analyze more precisely the forces exerted by the lined wall on the fluid.

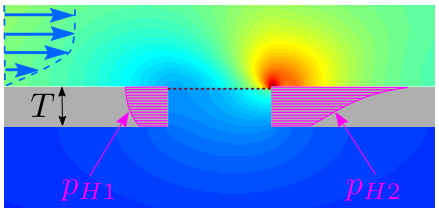

FIG. 6. (color online) Pressure field computed in a hole at 3600 Hz. The magenta curves (p_{H1} and p_{H2}) represents the pressure distribution on the vertical walls of the hole.

The acoustical effect of a lined wall with grazing flow cannot be described by a single quantity independent of the incident wave, like the wall impedance. At least two quantities are needed. The two quantities used in this Stress–Impedance model are the impedance and a friction factor which links the pressure to a tangential stress at the wall. Compared to the previous model given in [1], the use of a wall stress can help to better understand the mechanisms of momentum transfer between the flow and wall in the vicinity of an acoustic treatment.

Appendix A: Derivation of Eqs. (8) and (9)

Assuming that the length scale of the variation of p and ξ along the axis y are much larger than δ, these functions can be developed for $0 < y < \delta$ in $p(y) = p_w + p'_w\, y + \mathcal{O}(\delta^2\, p''_w)$ and $\xi(y) = \xi_w + \xi'_w\, y + \mathcal{O}(\delta^2\, \xi''_w)$ where the prime indicates a partial derivative along y. Integrating Eq. (6) from 0 to δ , yields, up to the order δ, to:

$$\int_0^\delta \partial_y p \,\mathrm{d}y = p_\delta - p_w = \int_0^\delta \Omega^2 \xi \mathrm{d}y = \int_0^\delta \Omega^2 \mathrm{d}y\, \xi_w \quad \text{(A1)}$$

Doing the same operation in the case where the flow is uniform up to the wall leads to

$$p_\delta - p_w^* = \delta \Omega_0^2\, \xi_w \quad \text{(A2)}$$

Eliminating p_δ from these two equation leads to:

$$p_w - p_w^* = \Omega_0^2 \int_0^\delta 1 - \left(\frac{\Omega}{\Omega_0}\right)^2 \mathrm{d}y\, \xi_w \quad \text{(A3)}$$

which is Eq. (8).

On the same way, integrating Eq. (7) from 0 to δ , yields, up to the order δ, to:

$$\xi_\delta - \xi_w = \int_0^\delta \left(\frac{k^2}{\Omega^2} - 1 \right) \mathrm{d}y \, p_w \tag{A4}$$

Doing the same operation in the case where the flow is uniform up to the wall leads to

$$\xi_\delta - \xi_w^* = \delta \left(\frac{k^2}{\Omega_0^2} - 1 \right) p_w \tag{A5}$$

Subtracting those two equations to eliminate ξ_δ leads to:

$$\xi_w - \xi_w^* = \frac{k^2}{\Omega_0^2} \int_0^\delta 1 - \left(\frac{\Omega_0}{\Omega} \right)^2 \mathrm{d}y \, p_w \tag{A6}$$

which is Eq. (9).

ACKNOWLEDGMENTS

This work was supported by the "Agence Nationale de la Recherche" international project FlowMatAc No. ANR-15-CE22-0016-01. The author benefits from fruitful discussions with J. Golliard, G. Gabard and X. Dai.

[1] Aurégan, Y., Starobinski, R., and Pagneux, V. (**2001**). "Influence of grazing flow and dissipation effects on the acoustic boundary conditions at a lined wall," The Journal of the Acoustical Society of America **109**(1), 59–64, doi: 10.1121/1.1331678.

[2] Bodén, H., Cordioli, J. A., Spillere, A. M., and Serrano, P. G. (**2017**). "Comparison of the effect of flow direction on liner impedance using different measurement methods," in *23rd AIAA/CEAS Aeroacoustics Conference*, p. 3184, doi: 10.2514/6.2017-3184.

[3] Brambley, E. J. (**2011**). "Well-posed boundary condition for acoustic liners in straight ducts with flow," AIAA journal **49**(6), 1272–1282, doi: 10.2514/1.J050723.

[4] Dai, X., and Aurégan, Y. (**2016**). "Acoustic of a perforated liner with grazing flow: Floquet-bloch periodical approach versus impedance continuous approach," The Journal of the Acoustical Society of America **140**(3), 2047–2055, doi: 10.1121/1.4962490.

[5] Ingard, U. (**1959**). "Influence of fluid motion past a plane boundary on sound reflection, absorption, and transmission," The Journal of the Acoustical Society of America **31**, 1035, doi: 10.1121/1.1907805.

[6] Khamis, D., and Brambley, E. J. (**2016**). "Acoustic boundary conditions at an impedance lining in inviscid shear flow," Journal of Fluid Mechanics **796**, 386–416, doi: 10.1017/jfm.2016.273.

[7] Khamis, D., and Brambley, E. J. (**2017**). "Acoustics in a two-deck viscothermal boundary layer over an impedance surface," AIAA Journal doi: 10.2514/1.J055598.

[8] Kopiev, V., Mironov, M., and Solntseva, V. (**2008**). "Aeroacoustic interaction in a corrugated duct," Acoustical Physics **54**(2), 197, doi: 10.1134/S1063771008020061.

[9] Myers, M. (**1980**). "On the acoustic boundary condition in the presence of flow," Journal of Sound and Vibration **71**(3), 429 – 434, doi: 10.1016/0022-460X(80)90424-1.

[10] Rebel, J., and Ronneberger, D. (**1992**). "The effect of shear stress on the propagation and scattering of sound in flow ducts," Journal of sound and vibration **158**(3), 469–496, doi: 10.1016/0022-460X(92)90420-3.

[11] Renou, Y., and Aurégan, Y. (**2011**). "Failure of the ingard–myers boundary condition for a lined duct: An experimental investigation," The Journal of the Acoustical Society of America **130**(1), 52–60, doi: 10.1121/1.3586789.

[12] Schlichting, H. (**1979**). *Boundary-layer theory*, 7 ed. (McGraw-Hill, New York).

[13] Schulz, A., Weng, C., Bake, F., Enghardt, L., and Ronneberger, D. (**2017**). "Modeling of liner impedance with grazing shear flow using a new momentum transfer boundary condition," in *23rd AIAA/CEAS Aeroacoustics Conference*, p. 3377, doi: 10.2514/6.2017-3377.

[14] Weng, C., Schulz, A., Ronneberger, D., Enghardt, L., and Bake, F. (**2017**). "Flow and viscous effects on impedance eduction," AIAA Journal 1–15, doi: 10.2514/1.J055838.

[15] Weng, C., Schulz, A., Ronneberger, D., Enghardt, L., and Bake, F. (**2017**). "Impedance eduction in the presence of turbulent shear flow using the linearized navier-stokes equations," in *23rd AIAA/CEAS Aeroacoustics Conference*, p. 3182, doi: 10.2514/6.2017-3182.

[16] Zhang, Q., and Bodony, D. J. (**2012**). "Numerical investigation and modelling of acoustically excited flow through a circular orifice backed by a hexagonal cavity," Journal of Fluid Mechanics **693**, 367–401, doi: 10.1017/jfm.2011.537.